

Short Communication

## **Sn<sup>4+</sup>-doped dendritic fibrous nanosilica (DFNS) nanoparticles as photocatalyst for degradation of rhodamine B**

Bangjun Han<sup>1</sup>, Qinli Lu<sup>2,\*</sup>, Jian Zhai<sup>1,\*</sup>, Renzheng Gu<sup>1</sup>

<sup>1</sup> School of Municipal and Ecological Engineering, Shanghai Urban Construction Vocational College, 200438 Shanghai, P. R. China

<sup>2</sup> School of Civil Engineering, Liaoning Petrochemical University, 113001 Fushun, P. R. China

\*E-mails: [hanbangjun@succ.edu.cn](mailto:hanbangjun@succ.edu.cn), [luqinli@lnpu.edu.cn](mailto:luqinli@lnpu.edu.cn), [zhaijian@succ.edu.cn](mailto:zhaijian@succ.edu.cn), [gurenzheng@succ.edu.cn](mailto:gurenzheng@succ.edu.cn)

Received: 3 August 2021/ Accepted: 18 September 2021 / Published: 10 November 2021

---

This work was done on synthesis of Sn<sup>4+</sup>-doped dendritic fibrous nanosilica (DFNS) nanoparticles (Sn-doped DFNS NPs) for photocatalytic degradation of rhodamine B (RHB) dyes as a chemical pollutant. The pure DFNS NPs and Sn-doped DFNS NPs were synthesized through a facile chemical method. The morphologies and crystal structures of the prepared specimens were studied using SEM and XRD analyses which indicated corrugated radial structure and confirmed the doping Sn ion into the DFNS lattice. Electrochemical characterization revealed that the enhancement of specific capacitance in electric double-layer due to the doping Sn ion into the DFNS lattice. The results of photocatalytic degradation of RHB revealed the 82.8% degradation of 40 mg/l of RHB in presence of Sn-doped DFNS NPs were obtained under 120 min visible-light irradiation. These findings exhibited that degradation efficiency of DFNS NPs was significantly improved by doping Sn ions in DFNS NPs under visible irradiation which can be attributed to the high specific surface area of Sn-doped DFNS NPs.

---

**Keywords:** Sn-doped dendritic fibrous nanosilica; Photocatalytic degradation; Rhodamine B; Electrochemical property; Visible-light irradiation

### **1. INTRODUCTION**

Dye pollutants of industrial wastewaters such as pulp, textiles, leather, soap, petrochemicals, plastics, palm oil, and chemicals can be released into natural ecosystem and polluted groundwater sources, lakes, agricultural soils, rivers and etc [1-3]. Studies have shown that industrial dyes are highly toxic and pose significant risks to the natural environment because of aromatic amino poisoning [4-6]. Nowadays, improper waste management and industrial development lead to an increase in organic pollutants in animals and human habitats and make significant health issues and carcinogenic effects [7, 8].

Among the various techniques being developed to deal with energy and environmental problems, photocatalysis offers several benefits such as easy reuse and complete elimination of dyes from wastewaters without harming the environment [9, 10]. Thus, photocatalysis is considered an efficient, green chemical, and promising method [11-13].

Nanomaterials are of interest to researchers due to their essential role in catalytic, optical, electrical, and magnetic applications [14-16]. However, the size-dependent property of semiconductors suggest a significant chance to produce a new device [17, 18].

Fibrous nano-silica (FNS) is a dendritic nanomaterial with exceptional physicochemical properties such as high surface area-to-volume ratio, low-toxicity and high-stability [19-21]. These features, along with its easy surface functionalization, provide opportunities to prepare more stable and highly sensitive bio-device [22, 23]. In addition to the durability of FNS-based material, this material is stable even under more severe conditions of higher pressures and temperatures where their morphologies remained unchanged [24, 25]. Lastly, purification and synthesis of FNS-based materials are easy and can be stored at room temperature for some techniques without any changes in its property [26-28].

Although numerous studies had been conducted to explore photocatalytic properties of nanomaterials, the Sn<sup>4+</sup>-doped dendritic fibrous nanosilica (DFNS) nanoparticles have never been considered before. Thus, this study was done on the fabrication of Sn-doped DFNS nanoparticles for photocatalytic degradation of dye pollutants. Furthermore, EIS and CV analyses were used to study the physical and chemical properties (especially the electrical conductivity) of the samples.

## 2. MATERIALS AND METHOD

Sn<sup>4+</sup>-doped dendritic fibrous nanosilica (DFNS) nanoparticles were synthesized as stated by the following steps. 4.5 mL of NaOH (2M) and 2.0gr of Cetyltrimethylammonium Bromide (CTAB) was added to 250mL of DI water and sonicated for 40 min. Next, 0.4 gr of tin (IV) chloride and 4.5mL of TEOS were added drop-wise into the mixture. After that, the prepared mixture was refluxed at 70°C for 1h. Then, the suspension was washed and filtrated several times with DI water and ethanol. Finally, Sn-doped DFNS was vacuumed for 3h and then calcinated at 450°C for 5h to eliminate the CTAB template.

The morphologies of prepared Sn<sup>4+</sup>-doped DFNS nanoparticles were studied through scanning electron microscopy (FESEM, FEI Sirion 200) and transmission electron microscopy (TEM, Philips CM12, FEI, CO) analyses. X-ray diffraction (XRD) was used to consider the crystal structure of prepared samples which was working at 25mA and 40kV in wavelength ( $\lambda=1.5418 \text{ \AA}$ ) of CuK $\alpha$ .

EIS and CV measurements were conducted by MetrohmAutolab tools in a traditional three-electrode electrochemical cell which included Ag/AgCl, Pt wire and, prepared Sn-doped DFNS electrodes as a reference electrode, a counter electrode and a working electrode, respectively. The electrolyte of CV analysis was 0.1M PBS which prepare by Na<sub>2</sub>HPO<sub>4</sub> (99.0%). For EIS test, the electrolyte solution was 0.5M Na<sub>2</sub>SO<sub>4</sub> (99%).

The photodegradation experiments were done for degradation of 40mg<sup>l</sup><sup>-1</sup> rhodamine B (RHB) on prepared Sn-doped DFNS photocatalysts. Before the dye degradation test, the photocatalysts and dye solution were held in dark for 40min to create the adsorption-desorption equilibrium. The tests were performed using a borosilicate glass flask reactor which was exposed to UV (500W, Halogen lamp, 420nm cut-off filter) and visible-light (23W) sources. Then, RHB solution was centrifuged at 2000rpm for 20min, and a spectrophotometer was utilized to recorded photo-degradation of RHB dye as the following equation:

$$\text{Degradation efficiency (\%)} = \frac{A_0 - A}{A_0} \times 100 \quad (1)$$

Where A and A<sub>0</sub> are the absorbance of RHB dye solutions after irradiation at any time t and initial absorbance, respectively.

### 3. RESULT AND DISCUSSION

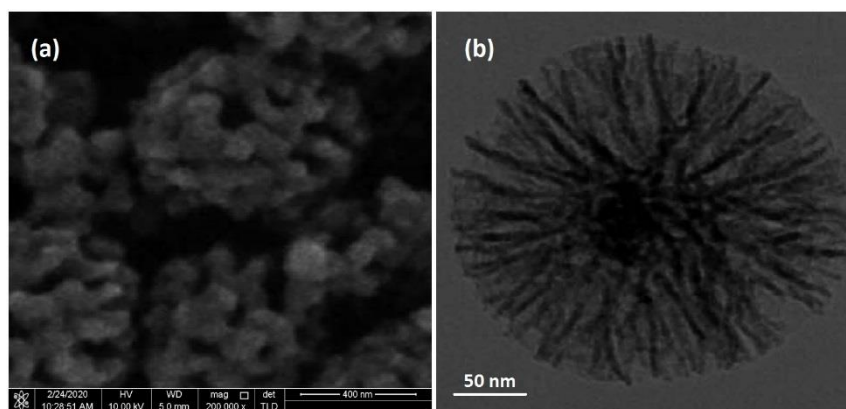


**Figure 1.** Morphologies of prepared Sn-doped DFNS NPs (a) SEM and (b) TEM

The morphology of prepared Sn-doped DFNS NPs were considered by SEM and TEM. Fig. 1 shows the SEM and TEM images of much textured spherical Sn-doped DFNS samples with a 300nm diameter and corrugated radial structure. As shown, the corrugated fiber (10nm) are protruded from the DFNS core and prepared radially in three physical dimensions. Overlapping the corrugated radial structures create open conical cavities [29]. The SEM image indicates the fibrous structure of the sphere and its solidity. Furthermore, the radial structure and fibers improve the entrance to active sites and enable the transport of chemicals.

The as-prepared DFNS and Sn-doped DFNS NPs were shown the crystalline nature. The XRD patterns were measured for the specimens. Figure 2 reveals the XRD patterns of the synthesized prepared DFNS and the Sn-doped DFNS NPs. As shown in Fig. 2, the characteristic broad diffraction peak centered on  $2\theta=23^\circ$  confirmed its amorphous nature of DFNS NPs [30]. The sharper peaks

obviously show the presence of DFNS. The pure DFNS peak was big compared to that of the Sn-doped DFNS sample.

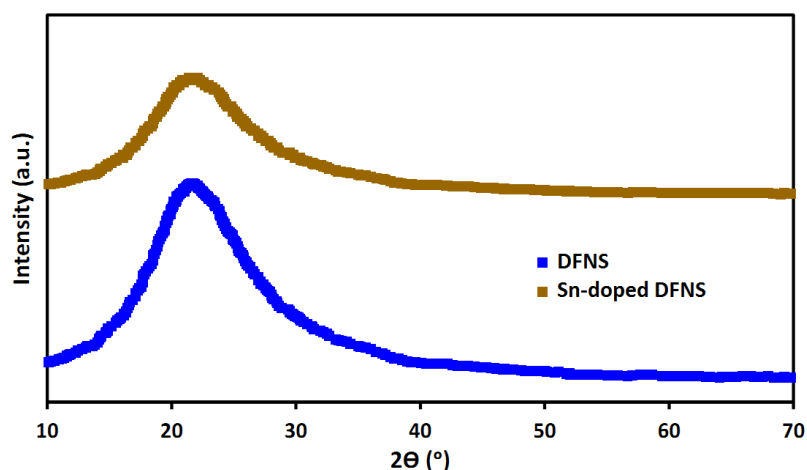


**Figure 2.** The XRD patterns of the synthesized prepared DFNS and Sn-doped DFNS NPs

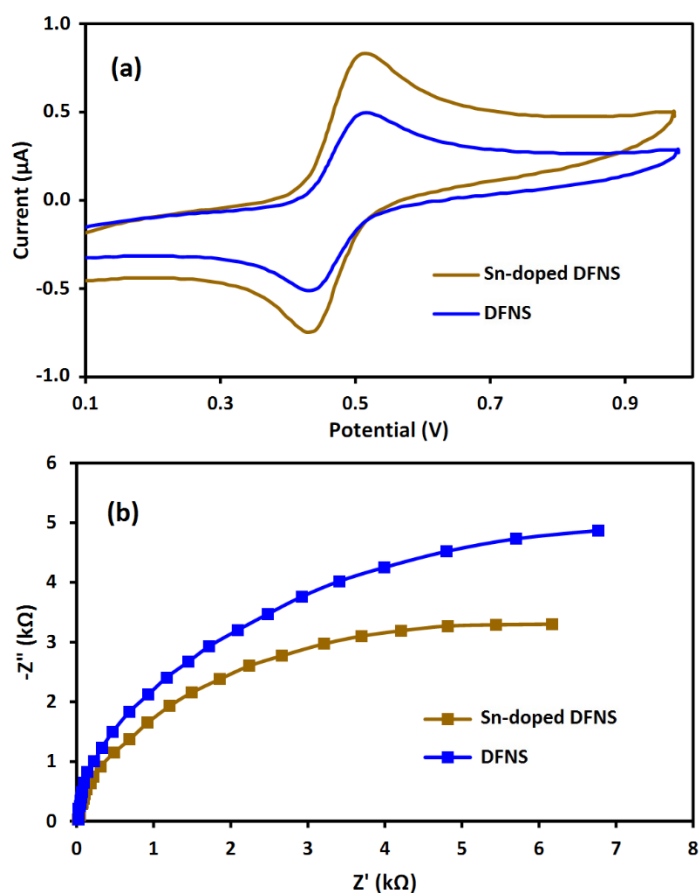


**Figure 3.** (a) CV results of prepared DFNS and Sn-doped DFNS NPs in 0.1M PBS solution at 10 mVs<sup>-1</sup> scan rate with 0.1-1.0 V potential range (b) Nyquist plots of prepared DFNS and Sn-doped DFNS NPs in frequency range of 0.1-10<sup>5</sup> Hz at an applied voltage of 10mV in 0.5M Na<sub>2</sub>SO<sub>4</sub> solution

Figure 3 indicates the recorded CVs of prepared DFNS and the Sn-doped DFNS NPs in 0.1M PBS solution at  $10 \text{ mVs}^{-1}$  scan rate with 0.1-1.0V potential range. As shown, Sn-doped DFNS sample reveals a greater surrounded area which shows the enhancement of specific capacitance in electric double-layer due to the doping Sn ion into the DFNS lattice. It can improve the value of charge storage and enhanced the electronic storage ability of Sn-doped DFNS toward pure DFNS NPs [31, 32]. EIS tests were done in the frequency range of 0.1- $10^5$  Hz at an applied voltage of 10mV in 0.5M  $\text{Na}_2\text{SO}_4$  solution. Fig. 3b indicates the Nyquist plots of specimens that was clearly shown smaller resistance of the Sn-doped DFNS NPs than pure DFNS NPs, which denote to enhance the DFNS's conductivity by doping Sn ions into DFNS because of the synergistic effect between DFNS and Sn nanostructures [33-35]. Moreover, a high electron-transfer rate may be associated with more interfaces between DFNS and Sn.

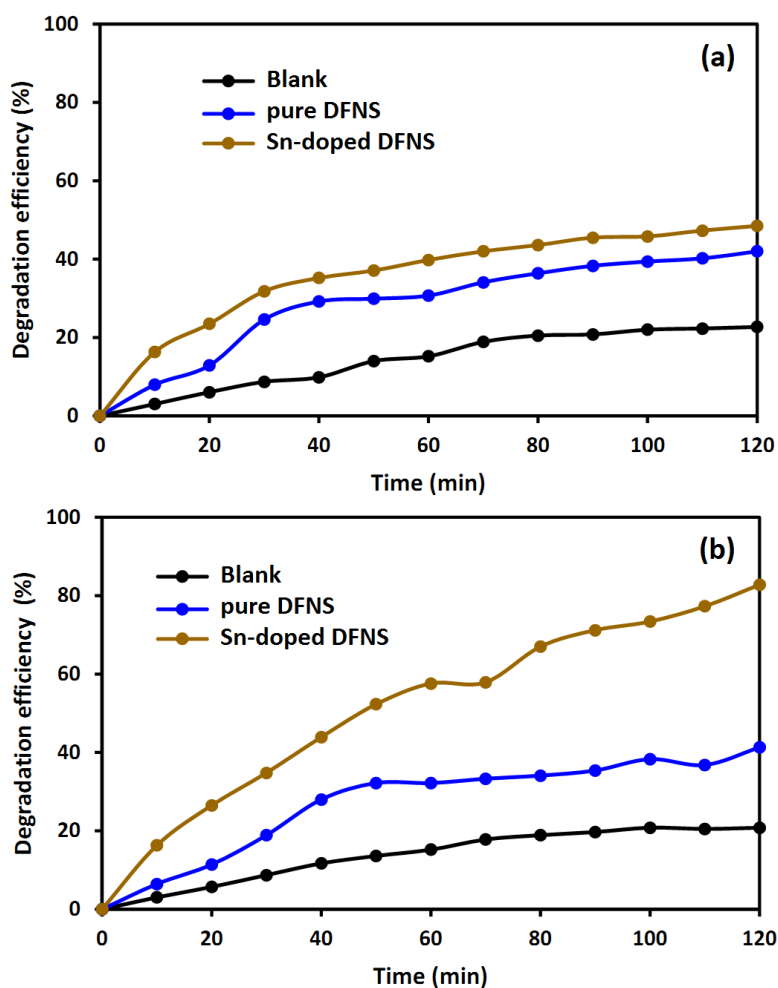


**Figure 4.** Degradation efficiency of prepared DFNS and Sn-doped DFNS NPs for RHB dyes under (a) UV-light (b) visible-light irradiation.

To assess the photocatalytic activities of prepared DFNS and Sn-doped DFNS NPs for the degradation of RHB under visible and UV lights irradiation. Fig.4 shows the degradation of RHB dye

in different conditions without catalysts (blank) and with pure DFNS photocatalyst and Sn-doped DFNS NPs films. As shown in figure 4, the blank displays 20.8% and 22.7% degradation efficiency after 120min irradiation of visible and UV lights, respectively. As observed, 41.3% and 42% degradation efficiency are for pure DFNS film under 120min irradiation of visible and UV lights, respectively which indicates photo-degradation activity increased under UV irradiation because of the band-gap values and photo-excited activity of DFNS under UV region. It is revealed 82.8% raise in the efficiency for Sn-doped DFNS NPs under 120min irradiation of visible light because of the high specific surface area of Sn-doped DFNS NPs [36]. According to the study of optical absorption, the interface effect of Sn ions and DFNS NPs can increase the transporting of the photo-generated carriers between two nanomaterials and reduce the recombination rate of photo-excited charges [37].

Photocatalytic activities are based on the creation of electron-hole pairs by the excitation of bandgap [38]. With visible light irradiation of Sn-doped DFNS NPs, DFNS could be studied as a sensitive nanostructure to absorb visible light. Afterward, the absorbed photon may generate the electron-hole pairs or may excite the electron of valence-band to the conduction band. This photo-excited electron can be trapped by joining an electron in the Sn conduction-band due to the vicinity of  $E_{VB}$  (valence band) of DFNS and Sn which decreases the recombination rate of the photo-excited electron. Furthermore, photo-generated holes remain in the DFNS surface. Thus, the photo-generated electron and hole can generate the hydroxyl radicals which may oxidize the adsorbed RHB molecules on the surface of the photocatalyst [39].

For further study on photocatalytic activities, the stability of Sn-doped DFNS films for degradation of RHB dyes was considered under visible-light irradiation. Fig. 5 displays that the photo-degradation efficiency reduces after 30min and 60min irradiation with increasing cycles. Besides, after 120min of visible-light irradiation, the degradation efficiency indicates stable activity for all five cycles.

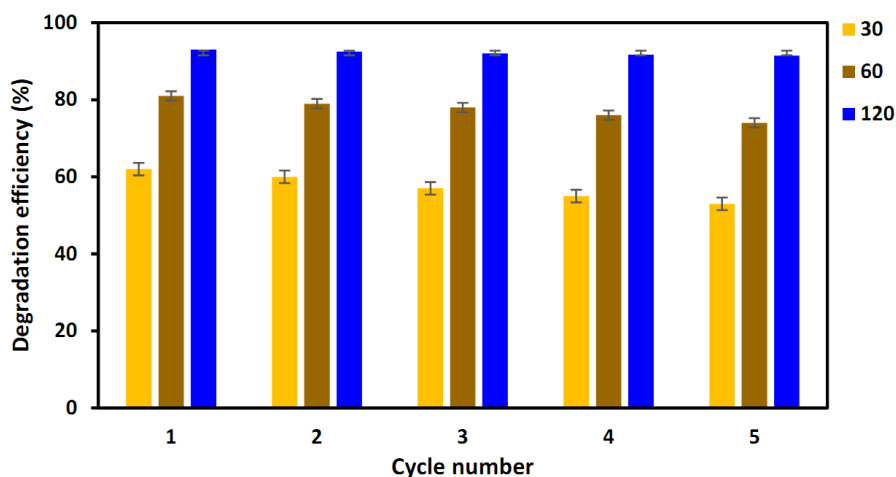


**Figure 5.** Cycling stability degradation tests of Sn-doped DFNS films for degradation of RHB dyes under visible-light irradiation for 30, 60 and 120min.

Table 1 shows the obtained findings of this work and other photocatalysts from literature for

degradation efficiency of RHB dyes. The comparison indicates great photocatalytic activity of Sn-doped DFNS NPs for degradation of RHB under visible irradiations which related to the synergistic effects of Sn ions and DFNS NPs which enables the electron-transfer in interface between DFNS and Sn. Moreover, the oxygen vacancies may promote charge separation into the Sn-doped DFNS NPs [40].

**Table 1.** Obtained findings of this work and other photocatalyst from literatures for degradation efficiency of RHB dyes

Photocatalyst	RHB content (mg/l)	Source	Degradation efficiency (%)	Degradation time (min)	Ref.
Sn-doped DFNS NPs	40.00	visible	82.8	120	This work
B/Sn-doped ZnO nanoparticle	20.00	visible	70.2	60	[41]
Sn-doped goethite nanocuboids	40.00	visible	70.0	120	[42]
Ce-doped ZnO	10.00	visible	97.6	120	[43]
LaFeO <sub>3</sub> -doped porous silica	10.00	visible	98.6	90	[44]
SiO <sub>2</sub> @C-doped TiO <sub>2</sub>	10.00	visible	61.7	60	[45]

#### 4. CONCLUSIONS

Here, the syntheses of Sn-doped DFNS nanoparticles for photocatalytic degradation of RHB dyes as a chemical pollutant were investigated. The pure DFNS NPs and Sn-doped DFNS NPs were synthesized through a facile chemical technique. The morphologies and crystal structures of the prepared specimens were studied using SEM and XRD analyses which indicated corrugated radial structure and confirmed the doping Sn ion into the DFNS lattice. Electrochemical characterization showed that the enhancement of specific capacitance in electric double-layer due to the doping Sn ion into the DFNS lattice. The results of photocatalytic degradation of RHB revealed the 82.8% degradation of 40 mg/l of RHB in presence of Sn-doped DFNS NPs were obtained under 120min visible light irradiation. These findings exhibited that degradation efficiency of DFNS NPs was significantly improved by doping Sn ions in DFNS NPs under visible irradiations which can be attributed to the high specific surface area of Sn-doped DFNS NPs.

#### References

1. M.F. Hanafi and N. Sapawe, *Materials Today: Proceedings*, 31 (2020) A141-A150.
2. D. Dutta, S. Arya and S. Kumar, *Chemosphere*, 285 (2021) 131245.
3. H. Karimi-Maleh, Y. Orooji, F. Karimi, M. Alizadeh, M. Baghayeri, J. Rouhi, S. Tajik, H. Beitollahi, S. Agarwal and V.K. Gupta, *Biosensors and Bioelectronics*, 184 (2021) 113252.
4. V. Mishra, U. Sharma, D. Rawat, D. Benson, M. Singh and R.S. Sharma, *Environmental research*, 184 (2020) 109253.
5. X. Xu and M. Nieto-Vesperinas, *Physical review letters*, 123 (2019) 233902.

6. Y. Orooji, B. Tanhaei, A. Ayati, S.H. Tabrizi, M. Alizadeh, F.F. Bamoharram, F. Karimi, S. Salmanpour, J. Rouhi and S. Afshar, *Chemosphere*, 281 (2021) 130795.
7. W. Li and V. Achal, *Science of the Total Environment*, 737 (2020) 139745.
8. D. Tan, H. Long, H. Zhou, Y. Deng, E. Liu, S. Wang and S. Zhang, *International Journal of Electrochemical Science*, 15 (2020) 12232.
9. N. Nasseh, L. Taghavi, B. Barikbin and M.A. Nasser, *Journal of cleaner production*, 179 (2018) 42.
10. P. Wang, L. Wang, H. Leung and G. Zhang, *IEEE Transactions on Geoscience and Remote Sensing*, 59 (2020) 2256.
11. R. Magudieswaran, J. Ishii, K.C.N. Raja, C. Terashima, R. Venkatachalam, A. Fujishima and S. Pitchaimuthu, *Materials Letters*, 239 (2019) 40.
12. Z. Li, Y. Shi, A. Zhu, Y. Zhao, H. Wang, B.P. Binks and J. Wang, *Angewandte Chemie International Edition*, 60 (2021) 3928.
13. H. Karimi-Maleh, M.L. Yola, N. Atar, Y. Orooji, F. Karimi, P.S. Kumar, J. Rouhi and M. Baghayeri, *Journal of colloid and interface science*, 592 (2021) 174.
14. J. Xu, X. Chen, Y. Xu, Y. Du and C. Yan, *Advanced Materials*, 32 (2020) 1806461.
15. X. Zhu, F. Lin, Z. Zhang, X. Chen, H. Huang, D. Wang, J. Tang, X. Fang, D. Fang and J.C. Ho, *Nano letters*, 20 (2020) 2654.
16. H. Liu, X.-X. Li, X.-Y. Liu, Z.-H. Ma, Z.-Y. Yin, W.-W. Yang and Y.-S. Yu, *Rare Metals*, 40 (2021) 808.
17. J. Zhu and Z. Jiang, *International Journal of Electrochemical Science*, 16 (2021) 210318.
18. X. Chen, D. Wang, T. Wang, Z. Yang, X. Zou, P. Wang, W. Luo, Q. Li, L. Liao and W. Hu, *ACS applied materials & interfaces*, 11 (2019) 33188.
19. M. Mahmudi, N. Shadjou and F.A.M. Hasanzadeh, *Journal of Electroanalytical Chemistry*, 848 (2019) 113272.
20. X. Yang, Q. Li, E. Lu, Z. Wang, X. Gong, Z. Yu, Y. Guo, L. Wang, Y. Guo and W. Zhan, *Nature communications*, 10 (2019) 1.
21. G. Chen, F. Zhang, Z. Zhou, J. Li and Y. Tang, *Advanced Energy Materials*, 8 (2018) 1801219.
22. P. Qin, M. Wang, N. Li, H. Zhu, X. Ding and Y. Tang, *Advanced Materials*, 29 (2017) 1606805.
23. S. Zhang, S. Zhao, S. Huang, B. Hu, M. Wang, Z. Zhang, L. He and M. Du, *Chemical Engineering Journal*, 420 (2021) 130516.
24. A. Maity and V. Polshettiwar, *ChemSusChem*, 10 (2017) 3866.
25. L. Zhang, M. Zhang, S. You, D. Ma, J. Zhao and Z. Chen, *Science of the Total Environment*, 780 (2021) 146505.
26. S. Azizi and N. Shadjou, *Heliyon*, 7 (2021) e05915.
27. L. Zhang, J. Zheng, S. Tian, H. Zhang, X. Guan, S. Zhu, X. Zhang, Y. Bai, P. Xu and J. Zhang, *Journal of Environmental Sciences*, 91 (2020) 212.
28. J.-Z. Cheng, Z.-R. Tan, Y.-Q. Xing, Z.-Q. Shen, Y.-J. Zhang, L.-L. Liu, K. Yang, L. Chen and S.-Y. Liu, *Journal of Materials Chemistry A*, 9 (2021) 5787.
29. C. Liu and J. Rouhi, *RSC Advances*, 11 (2021) 9933.
30. J. Sun, Z. Xu, W. Li and X. Shen, *Nanomaterials*, 7 (2017) 102.
31. H. Lv, X. Zhang, Y. Li, Y. Ren, C. Zhang, P. Wang, Z. Xu, X. Li, Z. Chen and Y. Dong, *Microchimica Acta*, 186 (2019) 1.
32. X. Wang, Z. Feng, B. Xiao, J. Zhao, H. Ma, Y. Tian, H. Pang and L. Tan, *Green Chemistry*, 22 (2020) 6157.
33. D.-J. Park, R. Rajagopal and K.-S. Ryu, *Journal of Industrial and Engineering Chemistry*, 83 (2020) 260.
34. X. Jing, H. Wang, X. Huang, Z. Chen, J. Zhu and X. Wang, *Food Chemistry*, 337 (2021) 127971.

35. H. Cheng, T. Li, X. Li, J. Feng, T. Tang and D. Qin, *Journal of The Electrochemical Society*, 168 (2021) 087504.
36. R. Abazari, A.R. Mahjoub, J. Shariati and S. Noruzi, *Journal of cleaner production*, 221 (2019) 582.
37. V. Madhavi and P. Kondaiah, *Applied Surface Science*, 436 (2018) 708.
38. W. Yu, J. Zhang and T. Peng, *Applied Catalysis B: Environmental*, 181 (2016) 220.
39. Y. Qin, Z. Sun, W. Zhao, Z. Liu, D. Ni and Z. Ma, *Nano-Structures & Nano-Objects*, 10 (2017) 176.
40. S. Jin, X. Ma, J. Pan, C. Zhu, S.E. Saji, J. Hu, X. Xu, L. Sun and Z. Yin, *Applied Catalysis B: Environmental*, 281 (2021) 119477.
41. A.Z. Ahmed, M.M. Islam, M.M.u. Islam, S.M. Masum, R. Islam and M.A.I. Molla, *Inorganic and Nano-Metal Chemistry*, 14 (2020) 1.
42. N. Popov, M. Ristić, M. Robić, V. Gilja, L. Kratožil Krehula, S. Musić and S. Krehula, *Chemical Papers*, 23 (2021) 1.
43. B. Hu, Q. Sun, C. Zuo, Y. Pei, S. Yang, H. Zheng and F. Liu, *Beilstein journal of nanotechnology*, 10 (2019) 1157.
44. T.T.N. Phan, A.N. Nikoloski, P.A. Bahri and D. Li, *RSC Advances*, 8 (2018) 36181.
45. Y. Zhang, J. Chen, L. Hua, S. Li, X. Zhang, W. Sheng and S. Cao, *Journal of hazardous materials*, 340 (2017) 309.

© 2021 The Authors. Published by ESG ([www.electrochemsci.org](http://www.electrochemsci.org)). This article is an open access article distributed under the terms and conditions of the Creative Commons Attribution license (<http://creativecommons.org/licenses/by/4.0/>).